Precision Agric (2012) 13:322–336
DOI 10.1007/s11119-011-9249-y

Sectioning remote imagery for characterization of *Avena sterilis* infestations. Part A: Weed abundance

David Gómez-Candón · Francisca López-Granados · Juan J. Caballero-Novella · Alfonso García-Ferrer · José M. Peña-Barragán · Montserrat Jurado-Expósito · Luis García-Torres

Published online: 6 November 2011

Abstract Software was developed to spatially assess key crop characteristics from remotely sensed imagery. Sectioning and Assessment of Remote Images (SARI®), written in IDL® works as an add-on to ENVI®, has been developed to implement precision agriculture strategies. SARI® splits field plot images into grids of rectangular "micro-images" or "micro-plots". The micro-plot length and width were defined as multiples of the image spatial resolution. SARI® calculates different indicators for each micro-plot, including the integrated pixel digital values. Studies on weed patches were done with SARI® using ground-truth data and remote images of two wheat plots infested with *Avena sterilis* at LaFloridaII and Navajas (Southern Spain). Patches of *A. sterilis* represented 47.5 and 19.2% of the field areas at the two locations, respectively; the infested areas were a combination of a few large and several small patches. At LaFloridaII, 2.1% of all patches were >500 m^2 and 55.0% of all patches were smaller than 10 m^2. Based on ground-truth weed abundance data, SARI® output includes geo-referenced and visual herbicide prescription maps, which could be used with variable-rate application equipment.

Keywords SARI® add-on software · Remote sensing · Weed spatial distribution · Herbicide prescription maps

Nomenclature

Wild oat	*Avena sterilis* sp. *sterilis* L.
Wheat	*Triticum durum* L.

D. Gómez-Candón · F. López-Granados · J. J. Caballero-Novella · J. M. Peña-Barragán · M. Jurado-Expósito · L. García-Torres (✉)
Institute for Sustainable Agriculture, CSIC, Apartado 4084, 14080 Cordoba, Spain
e-mail: lgarciatorres@ias.csic.es

A. García-Ferrer
Faculty of Agriculture and Forestry, University of Cordoba, Campus of Rabanales, Cordoba, Spain

Introduction

Site-specific agriculture takes into account the spatial variability of biotic factors, such as weeds and pathogens, and of abiotic factors, such as nutrients or water content. Additionally, it uses diverse technologies to apply fertilizers, pesticides or other inputs at variable rates, fitting the needs of each defined area (Blackmore 1996; Kropff et al. 1997). The patchy distribution of weeds in fields has been observed and is well documented (e.g. Jurado-Expósito et al. 2003; Krohmann et al. 2006). However, herbicides are usually applied at a single rate over an entire field. To reduce the total amount of herbicide sprayed, site-specific weed management (SSWM) techniques are being developed, allowing pesticide application only where weed densities exceed the economic threshold and reducing application rates in patches where weed densities are low (Christensen et al. 2003; Barroso et al. 2004, 2005). Potential economic and environmental benefits of SSWM include reduced spray volume, decreased application time and lower non-target spraying (Thompson et al. 1991; Medlin et al. 2000). The economic benefits of SSWM have proved to be potentially high for various crops in experimental studies (Timmermann et al. 2003). Although proximal "on-the-go" sensors in cereal crops are used commercially to maximise farmer's profit, the use of remote sensing in precision agriculture is still in a developmental phase. Several technological constraints, such as accurate and automatic image georeferencing, calibration and splitting larger images into micro-images, and assessment strategies, need to be overcome (García-Torres et al. 2010).

Spectral reflectance differences can be enhanced by using ratios or linear combinations of bands or selected wavelengths when multi-spectral (visible and near infrared spectral bands) and hyperspectral (over 6–8 spectral bands) data are used, respectively. The ratios take advantage of vegetation reflectance contrast between different wavelengths. Usually, vegetation indices give an indication of the presence or absence of vegetation but not of weed species. The most widely used indices in multi-spectral remote sensing are: the Normalized Difference Vegetation Index (NDVI: NIR − R/NIR + R; Rouse et al. 1973), and the Ratio Vegetation Index (RVI: NIR/R; Jordan 1969). NDVI and RVI are commonly used to differentiate vegetation because it usually shows high reflectance in NIR and low in R, and both indices enhance these differences (Koger et al. 2003). In some reports, multispectral information and NDVI were used to discriminate *Panicum effesum* R. Br. in oilseed rape (*Brassica napus* L.) stubble (Lamb and Weedon 1998), wild oat in wheat triticale (Lamb et al. 1999), yellow hawkweed (*Hieracium pratense* Tausch) and oxeye daisy (*Chrisanthemum leucanthemum* L.) in pastures and meadows (Lass and Callihan 1997), yellow starthistle (*Centaurea solstitialis* L.) (Lass et al. 2000), and weed-free and weed-infested areas in soybean (Chang et al. 2004). Similarly, in previous works, our group has described the mapping of late-season infestations of *Avena sterilis* in wheat (López-Granados et al. 2006), of *Ridolfia segetum* Moris in sunflower (*Helianthus annuus* L.) (Peña-Barragán et al. 2007), and of cruciferous weeds in wheat and legumes (deCastro et al. 2009) using remote sensing. Detection of late-season weed infestations with remote sensing is feasible when plants are mature, the soil surface is completely covered and the influence of background soil and crop residue reflectance is minimum (Koger et al. 2003). Thus, taking into account that weed infestations can be relatively stable from year to year (Wilson and Brain 1991), late-season weed detection maps can be used to design site-specific control methods in the following years. Other works support the idea that weed management systems do not require differentiation between weed species, but rather between crop and other vegetation for using non-selective herbicides or combination of grass and broadleaf herbicides (Vrindts et al. 2002), or among crop and monocotyledonous

and dicotyledonous weeds for reducing non-target spraying (Gibson et al. 2004; Thorp and Tian 2004).

Wild oat (*Avena sterilis* sp. *sterilis* L. AVEST) is the most common grass weed in winter cereal crops and is found in 65% of the arable fields in Southern Spain (Saavedra et al. 1989). Wheat (*Triticum durum* L., *T. aestivum* L.) is a very important crop in many countries and over 5 M ha are grown annually in Spain (MARM 2011). Barroso et al. (2004) studied the patchy distribution and spatial stability of *A. sterilis* in long-term field experiments and concluded that the location of the infestation was quite stable throughout a 5-year period. The abundance and distribution of *A. sterilis* in dry land barley fields was studied in several Spanish provinces and it was concluded that most infestations were concentrated in a few large but unevenly-shaped patches, with a larger number of smaller and more even patches accounting for a small proportion of the infestation (Ruiz et al. 2006). Taking into account that *Alopecurus myosuroides* and *A. sterilis* weed infestations can be relatively stable from year to year (Wilson and Brain 1991; Barroso et al. 2004), late-season weed detection maps can be used to design SSWM for the subsequent years. A further aim of weed patch mapping is to design a prescription herbicide application map and, for this purpose, the spatial resolutions of patch mapping and subsequent spraying have turned out to be critical parameters for SSWM implementation. For practical reasons, these spatial resolutions need to be matched (Ruiz et al. 2006).

Cost–effective large-scale mapping of biotic/abiotic parameters needs to be developed to take full advantage of SSWM. Software to manage remotely sensed images can play an important role in the fulfilment of this objective. The aim of this work was to develop software to manage remotely sensed images for site-specific agricultural applications, so-called Sectioning and Assessment of Remote Images (SARI®), and to show the usefulness of the software for winter wheat infested with *A. sterilis* patches. The specific objectives of this study were as follows: (1) to describe the development of SARI® software, (2) to show quantitative information provided by SARI® and herbicide prescription map, and (3) to use the software to assess weed patches, grouping them according to infestation level.

Materials and methods

Image processing requirements: ENVI, IDL and SARI®

ENVI® 4.6 (Visual Information Solution Inc., Boulder, Colorado, USA) was the computer program used for visualizing and processing images; this is written in IDL®, a systematized computer language that permits integrated image processing (Visual Information Solution Inc., Boulder, Colorado, USA). To achieve the objective of this paper, our research group has developed the software named SARI®, which is also written in IDL and works as an add-on to ENVI.

SARI® software

This has been developed to implement precision agriculture strategies (García-Torres et al. 2008a, 2009). SARI® splits field plot images into grids of rectangular "micro-images" or "micro-plots", whose length and width are arbitrarily defined as multiples of the spatial resolution of the image. SARI® calculates various indicators for each micro-plot, such as the integrated pixel digital values (IDV) and the percentage of pixels (%PI) with digital

value (DV) $\neq$ 0, and then classifies the micro-plots into arbitrarily defined classes based on these indicators.

Land uses classification

Any waveband or vegetation index image in which land uses can be discriminated was suitable for processing by SARI®. First, a supervised classification of the main land uses in the image is needed to define the boundary digital values (BDV), which characterize each identified land use and the accuracy statistics of the classification. The BDV of the selected land uses, among other parameters, will be subsequently implemented in the SARI® software. In the classification process, the statistics commonly used are the overall accuracy (OA) and Kappa coefficient (KC); OA and KC of over 85–90% and 0.80–0.85, respectively, are generally recommended (Landis and Kock 1977; Thomlinson et al. 1999).

SARI definition parameters

Once a remotely sensed image has been selected, a set of parameters need to be obtained and introduced into SARI®'s main interface:

(a) *Clustering parameters* are needed to characterize the patches and are defined as follows:

- a.1 Boundary digital values (BDV): define the selected land use Maximum BDV (BDV_{MAX}) and Minimum BDV (BDV_{MIN}) and should be obtained by applying a main land use classification process as previously described.
- a.2 Cluster merging distance (CMD): maximum distance in between patches or clusters required to merge neighbouring patches or clusters, which are defined in pixels. In clustering studies, CMD was considered a variable to be analysed.
- a.3 Minimum Clustering Size (CS_{MIN}): any patches or clusters smaller than the defined size (in number of pixels) were discarded and not taken into account for further calculations.
- a.4 Clustering Size (CS_{MAX}): defines a maximum number of columns (Width, W_{CMAX}) and rows (Length, L_{CMAX}) to keep in a cluster; patches with higher values than these maxima are split into smaller clusters.

(b) Region of Interest (ROI) was the grid size or micro-plot parameters of the sectioned image defined as follows:

- b.1 The maximum number of columns (Width, W_{RMAX}) and
- b.2 The maximum number of rows (Length, L_{RMAX}) in the regions of interest (ROI).

Each micro-plot is created in the geometric centre of each cluster.

Clustering pixels by SARI®

To cluster pixels into patches, SARI® operates by integrating the DVs of neighbouring pixels into a defined range of DV and the clustering dimension, which is given by a maximum number of columns (Width, W_{CMAX}) and a maximum number of rows (Length, L_{CMAX}). SARI® applies a mask over the processed image, using the range of BDV

(BDV_{MIN}, BDV_{MAX}) for each land use obtained in the overall land use classification procedure. The DV of every pixel of the image not belonging to the BDV range defined for the selected land use are fixed at 0, and the DV are retained for the pixels belonging within the BDV range. The next step is the determination of the clusters over the selected image. For SARI®, clusters are defined as groups of adjacent pixels in the size range defined. SARI® operates pixel by pixel, starting row by row from top to bottom and then column by column from left to right. A new identification number or name (label) is assigned to each pixel not connected to previously found clusters; otherwise, if it is connected, the assigned label will be the same. The distance allowed between clusters is defined by the CMD, where adjacent clusters located less than the CMD are merged. The cluster size range and the minimum (CS_{Min}) and maximum (CS_{Max}) clustering size are implemented, in order to discard clusters with a very large or small size in relation to the ROI.

Image splitting and micro-plot classification

The original image is divided into small images ("micro-images" or "micro-plots"), each of a size equal to the ROI defined by inputting clustering and ROI size parameters ($W_{CMAX} = W_{RMAX}$, $H_{CMAX} = H_{RMAX}$) into SARI®. Each ROI defined by SARI® exhibits all the quantitative information provided by the ROI menu of ENVI through the Statistics Sub-menu, for example, the number of pixels, mean and range of DVs. Similarly, the micro-images created by SARI® can be visually assessed in the original image and/or independently separated through other ENVI menus (Subset Data via ROI).

Each micro-plot MPi defined by SARI® is characterized with different parameters, as follows:

- X_i, Y_i, Geographic co-ordinates of micro-plot centre i.
- MPxi, Number of pixels of micro-plot i,
- IDVi, Accumulated digital value calculated as the arithmetical sum of all DV_s; $IDVi = \sum_i DVi$
- ADVi: Average digital value of the micro-plot i, $ADVi = IDVi/MPxi$
- IPN: Number of pixels of all micro-plots; $IPN = \sum_1^C MPxi$, c being the number of micro-plots,
- NOPIi, Number of pixel of micro-plot i with $DV \neq 0$
- % PIi, % of pixels of micro-plot i with $DV \neq 0$
- Class: Micro-plots can be classified as %PIi or %IDVi over the maximum of a selected micro-plot. The resulting classes correspond to previously established percentages of pixels as defined in the interface; for example: classes 0, 1, 2, 3, 4 and 5 could be equal to 0, 1–20, 21–40, 41–60, 61–80 and 81–100%, respectively, or to the selected percentage that is indicated.

The operational flowchart of SARI® is shown in Fig. 1.

Field locations, airborne images and processing

Remotely sensed images were obtained from a 1.95 ha portion of LaFloridaII farm (Utrera, Seville) and in a 2.69 ha portion of the Navajas farm (Sta. Cruz, Cordoba) in Southern Spain. Geographic co-ordinates of the upper left corner were $X = 242\,061$ m, $Y = 4\,124\,806$ m; and $X = 360\,870$ m, $Y = 4\,185\,307$ m (Universe Transverse Mercator system, zone 30 North, UTM-30N), respectively. In both locations, winter wheat

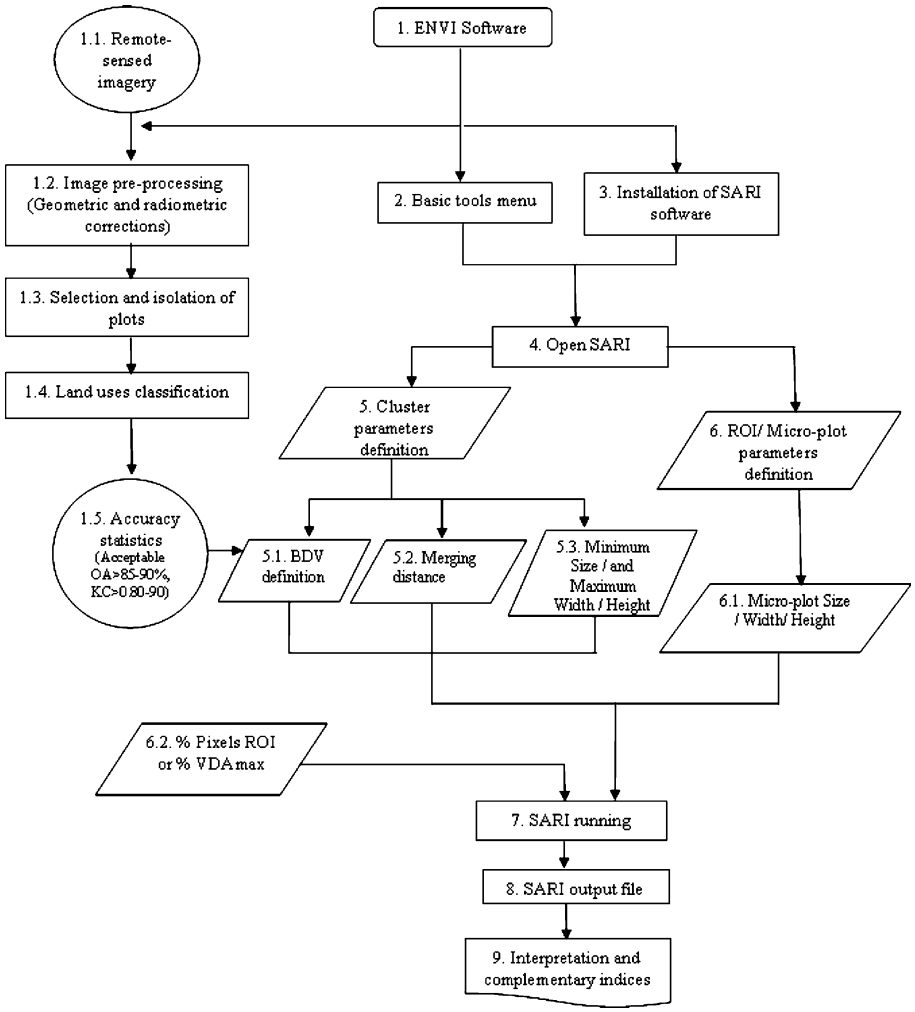

Fig. 1 SARI® operations flowchart; ▭ software initialization, ▭ main processes/sub-processes, ○ additional information, ▱ parameters inserted by the user, ▭ data outcome of SARI execution

(*T. durum* L. cultivar Mexicali) was sown in mid-November, 2005 at 140 kg ha^{-1}, and harvested early in June, 2006, and the fields were naturally infested with *A. sterilis*. Multi-spectral band colour-infrared KODAK film photographs (green, G: 500–600 nm; red, R: 600–700 nm; near infrared, NIR 700–1 100 nm) (Eastman Kodak Co., Rochester, New York, USA) were taken in mid-May, 2006 at noon. At this time, wheat plants were at an advanced stage of senescence and yellowing, while the *A. sterilis* panicles were at an advanced stage of seed maturation and partly green, corresponding to stages 92 and 83, respectively, as described by Lancashire et al. (1991). Photographs were taken from a turbo-prop twin-engine plane CESSNA 421 with WILD RC-30 photographic equipment. Flight altitude was 1 500 m, and photographs had an average scale of 1:10 000. Selected photographs were digitized using a Hewlett Packard ScanJet 4C scanner to obtain pixels of

0.5 and 1 m. Supervised classification of the grassy weed patches in wheat was previously described by López-Granados et al. (2006), who recommended the use of the NDVI index due to the high per-class accuracies obtained (0.87–0.94) in all locations.

Ground truth data

Each farm was visited during mid-May 2006 to assess visually ground-truth crop areas of several categories of weed abundance: (a) *A. sterilis*-free, (b) low (1–30 *A. sterilis* panicles m^{-2}, average 20 m^{-2}), (c) intermediate (31–80 panicles m^{-2}, average 60 m^{-2}), and (d) high infestation (>81 panicles m^{-2}, average 140 m^{-2}). About 10–12 selected crop areas measuring 2–3 m^2 of each weed density category were collected as training pixels for the development of threshold level, and a similar number of points of each category for the accuracy assessment. In addition, about 50 ground control points, namely singular points such as fence lines and lanes, were also geo-referenced in each farm to ensure accurate geographical co-ordinates of the images. Weed abundance areas and control points were geo-referenced using a sub-meter differential GPS TRIMBLE PRO-XRS (Trimble Navigation Limited, California, USA) and then overlaid onto the remotely sensed images using PATHFINDER OFFICE 2.51 software (Trimble Navigation Limited, California, USA). In the NDVI image of LaFloridaII and Navajas, BDV of each weed density category was defined from the corresponding ground-based geo-referenced points through an iterative process with a set of threshold BDV interval. To avoid any subjective estimation, each set of BDV was checked through a numerical confusion matrix analysis. The OA and KC of the whole classification process were calculated.

Quantitative information and herbicide prescription map provided by SARI®

To show the basic output and prescription map achieved by SARI®, the NDVI image of Navajas (Fig. 2a) was processed under the following specifications: BDV_{Min} and BDV_{Max} of 0.16 and 0.55, respectively, with no merging of clusters (Merging Distance = 0), no minimum cluster size limitation ($CS_{Min} = 1$), and CS_{Max} of 20 × 13 pixels and micro-plots size of 20 × 13 pixels. The classification criteria of the resulting micro-plots was % of pixels with class 1, 2 and 3, corresponding to <11, 11–26, and >26% infested pixels, respectively.

Weed patch assessment

SARI® software was used to determine weed patches (DV: 0.56–0.79) of over 1 pixel ($CS_{Min} = 1$), with no limitation on the maximum size (CS_{Max} Width and Length <10 000), grouped by area into the following classes: <3, 3–10, 11–50, 51–100, 101–500, 501–1 000 and >1 000 pixels. The number, mean size and its standard deviation, and total area of the patches of each class were determined based on different merging distances between patches of 1, 2, 3, 5 and 10 pixels.

Visually, weed patches were not uniform in infestation intensity (Fig. 2a). To show the capacity of SARI® for determining zones of similar weed density, two selected patches of 50 m × 50 m were isolated at LaFloridaII farm (Fig. 3). BDVs of the weed abundance categories were based on the geo-referenced ground-truth points. The area of each infestation zone was calculated by SARI® by using BDV with no limitation of cluster size and no merging of clusters.

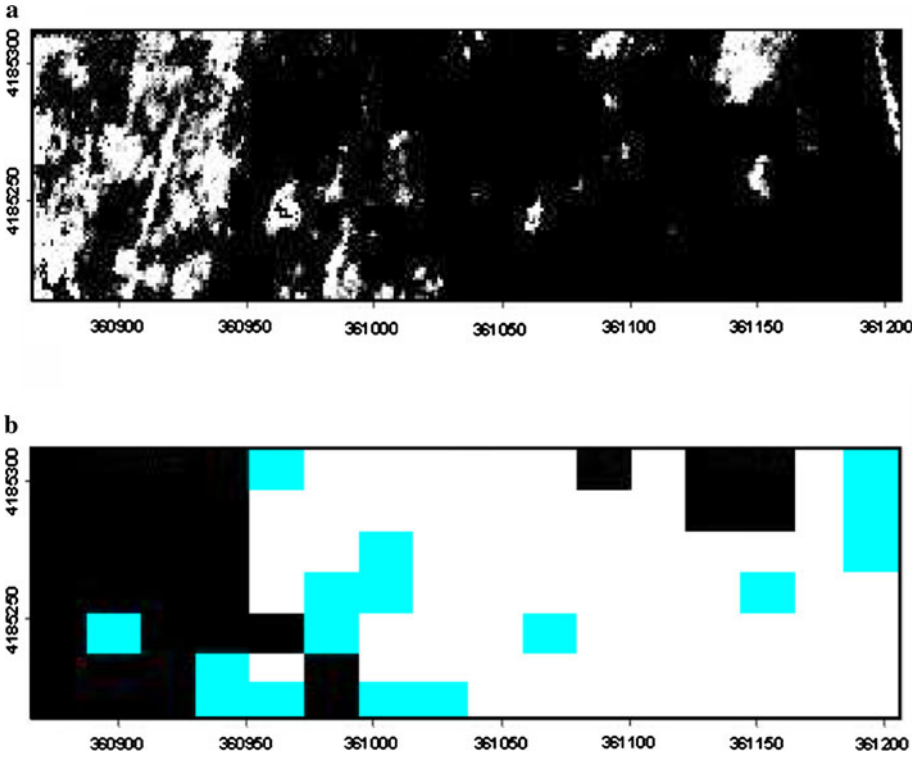

Fig. 2 **a** NDVI image view of Navajas (320 × 91 m) where wheat crop is shown in black (NDVI values <0.16) and wild oat patches in white (NDVI values 0.16–0.55); overall classification accuracy and Kappa coefficients were 84.8% and 0.78; and **b** herbicide prescription map: image processing characteristics and micro-plot classification criteria are described in the SARI Software section of the text. Low (<11% infested pixels), intermediate (11–26%) and high (>26%) weed intensity classes correspond to *white*, *cyan*/*grey* and *black colours*, respectively. Micro-plot size is 20 × 13 m. Geographic coordinates (UTM-30N) are indicated in meters (Color figure online)

Results

Weed abundance categories

The mean NDVI values and the selected BDV of weed free, very low/low, intermediate and high weed pressure categories were <0.56, 0.56–0.66, 0.67–0.72 and 0.73–0.80 for LaFloridaII, respectively, assessed with an overall classification accuracy (OA) of 93.6% and KC of 0.89 (Table 1). For the same categories at Navajas, the defined BDVs were <0.16, 0.16–0.39, 0.40–0.46 and 0.47–0.59 (Table 1), with an OA 84.8% and KC 0.78, respectively.

Quantitative information and herbicide prescription map provided by SARI®

The basic output and prescription maps provided by SARI® for the selected field plot at Navajas are shown in Table 2 and Fig. 2b, respectively. The original image was sectioned into 112 micro-plots of 20 × 13 pixels. The output of each micro-plot provided by SARI®

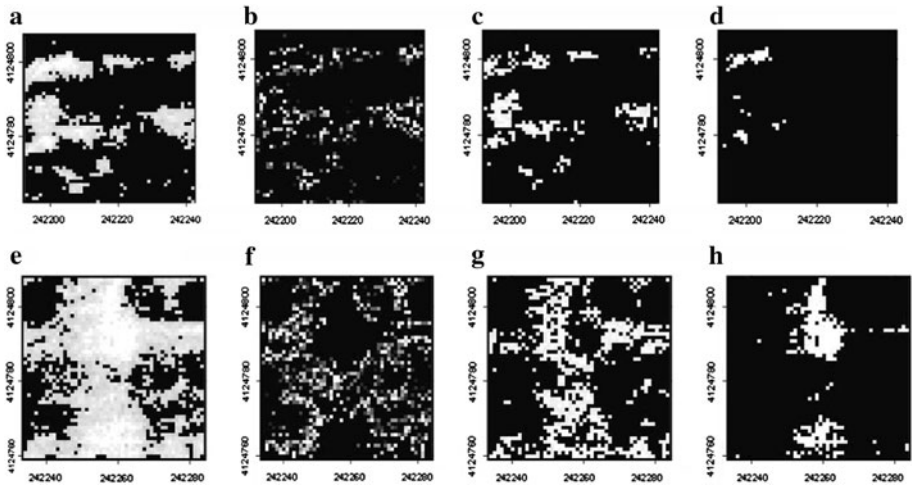

Fig. 3 View of the two selected wild oat patches of LaFloridaII (**a**–**d** and **e**–**h**) classified by infestation intensity: **a**, **e** overall (NDVI values 0.56–0.80); **b**, **f** low (0.56–0.60); **c**, **g** intermediate (0.61–0.67); and **d**, **h** high (0.68–0.8). *Black pixel* are *Avena*-free crop; *white pixel* are *Avena*-infested crop; the whiter the pixel, the higher the DV values, indicating high *Avena* infestation. Geographic coordinates (UTM-30N) are indicated in meters

gives its geographic location and key parameters such as the integrated digital values of each cluster (IDV), the number of pixels of each micro-plot (MPX) and their relationship IDV/MPX, among others (Table 2). Each micro-plot was also classified by the % infested pixels, such as <11, 11–26, and >26% infested pixels, for the classes 1, 2, and 3, respectively (Table 2). These micro-plot classifications can then be visualised as the site-specific prescription map (Fig. 2b).

Weed patch assessment

Avena sterilis patches were 47.5 and 19.2% of total area at LaFloridaII and Navajas, respectively. The number and area of weed patches at LaFloridaII was influenced by merging distance between patches (Table 3). The total number of patches with no merging was 227. Patch size distribution consisted of a few large patches and many small patches (Table 3). Merging of neighbouring patches consistently decreased the number of patches and increased their size. For example, the total number of patches decreased from 227 to 72 and 49 as merging distance increased from 1 to 2 to 3 pixels, respectively. It can be concluded that most patches were separated from each other by a few pixels, usually less than 3 m. Thus, the distance between patches considered greatly influenced the resulting number of patches and their average size. A similar numerical distribution of patches occurred at Navajas farm (data not shown for abbreviation).

SARI® efficiently quantified the zones of similar weed density within patches of each micro-plot. For example, for the two selected patches of LaFloridaII previously indicated (Fig. 3a–h), the zones classified as weed-free, low, intermediate or high infestation were 75, 12, 10 and 2% of their total area for patch #1, and 14, 23, 25 and 36% for patch #2, respectively. High *A. sterilis* densities usually occurred in the centre of the patches, thus coinciding with high DV; *A. sterilis* densities normally decreased from the centre of the patches to the *A. sterilis*-free zones, and so the corresponding DV decreased.

Table 1 Mean NDVI values and selected boundary digital values (BDV) for *Avena sterilis* abundance categories in wheat

Location	Categories									
	None/free		Low		Intermediate		High		Statistic	
	Mean	BDV	Mean	BDV	Mean	BDV	Mean	BDV	OA (%)	KC
LaFloridaII	0.16 ± 0.09	0.1–0.55	0.56 ± 0.17	0.56–0.66	0.70 ± 0.02	0.67–0.72	0.74 ± 0.02	0.73–0.80	93.6	0.89
Navajas	0.06 ± 0.07	−0.20–0.16	0.30 ± 0.1	0.16–0.39	0.41 ± 0.06	0.40–0.46	0.51 ± 0.11	0.47–0.59	84.8	0.78

BDV boundaries digital values, *OA* overall accuracy, *KC* Kappa coefficient

Table 2 Quantitative information provided by SARI® as Excel files for the sectioning of Navajas plot (Fig. 2a)

Micro-plot[a]	Coordinates		Pixel micro-plot^{-1}	Integrated digital values	Averaged digital values	Classification pixel DV ≠ 0		
	X	Y				No. of pixels.	% Pixel	Class
1	360 881	4 185 307	260	52.5	0.20	182	70.0	3
2	360 898	4 185 318	260	16.1	0.06	72	27.6	3
3	360 915	4 185 328	260	41.3	0.16	168	64.6	3
4	360 932	4 185 339	260	48.3	0.19	174	66.9	3
5	360 949	4 185 349	260	7.0	0.03	35	13.4	2
6	360 966	4 185 360	260	3.1	0.01	17	6.5	1
⋮	⋮	⋮	⋮	⋮	⋮	⋮	⋮	⋮
⋮	⋮	⋮	⋮	⋮	⋮	⋮	⋮	⋮
107	361 090	4 185 349	260	0.0	0.00	0	0.0	1
108	361 107	4 185 360	260	0.0	0.00	0	0.0	1
109	361 124	4 185 370	260	0.0	0.00	0	0.0	1
110	361 141	4 185 381	260	0.0	0.00	0	0.0	1
111	361 158	4 185 391	260	0.0	0.00	0	0.0	1
112	361 174	4 185 401	260	0.0	0.00	0	0.0	1
Overall image pixels	27 348	Digital values (DV)	Overall	1439.0				
			Average pixel^{-1}	0.05				

Processing characteristics and micro-plot classification criteria are described in the text

[a] Only data of the first and last six micro-plots are shown out of a total of 112 micro-plots

Discussion

Remotely sensed images cover large areas, ranging from several hundred hectares to dozens of square kilometres. Agricultural operations such as sowing, fertilization and pesticide applications are designed for field areas of smaller size, such as 20–30 ha, or with a high level of detail as with precision agriculture. In order to use remote sensing for agriculture, the first step is to isolate the image of the field in which to implement the desired action. Consequently, planning site-specific operations by remote sensing requires the isolated plot image to be sectioned into small micro-plots, for example of about 50–200 m^2, and then interpreting the appropriate agro-environmental indicator for the desired operation at each micro-plot. CLUAS® software was developed to programme site-specific actions for orchards and tree plantations by automatically determining agro-environmental indicators of each individual tree or small area (García-Torres et al. 2008b). The study has shown that similar actions can be planned using SARI® in agricultural plots where annual crops are growing. This software is effective in sectioning images and assessing key agro-environmental characteristics of each micro-plot, regardless of the size of the original image. Thus, SARI® meets one basic requirement of precision agriculture; that is, characterizing the needs of each small defined area

Table 3 Quantitative assessment of *Avena sterilis* weed patches identified by SARI® with an NDVI image from LaFloridaII affected by merging distance between patches

Merging distance (m)[a]	Overall patches		Patch size (m^2)							
			5 000–10 000	1 000–5 000	500–1 000	100–500	51–100	11–50	3–10	<3
1	Number	227	–	1	4	8	28	58	102	23
	%	100	–	0.4	1.7	3.5	12.3	25.5	44.9	10.1
	% Of total area[b]	–	–	11.2	30.1	19.3	17.5	15.0	5.6	0.6
	Mean size (m^2)	–	–	1 067 ± 0[c]	715 ± 125	234 ± 110	72 ± 15	24 ± 10	5 ± 2	2 ± 0
2	Number	72	–	2	3	5	7	23	26	6
	%	100	–	2.7	4.1	6.9	9.7	31.9	36.1	8.3
	% Of total area[a]	–	–	49.7	25.5	10.8	5.2	6.7	0.2	0.01
	Mean size (m^2)	–	–	2 362 ± 1 231	817 ± 98	206 ± 121	70 ± 12	27 ± 12	5.7 ± 2.4	2.0 ± 0
3	Number	49.0	–	2	4	4	6	11	16	6
	%	100	–	4.0	8.1	8.1	12.2	22.0	32.4	12
	% Of total area[a]	–	–	59.0	27.3	5.2	4.1	3.1	0.9	0.1
	Mean size (m^2)	–	–	2 807 ± 1 269	649 ± 117	163 ± 21	65 ± 17	27 ± 9	6 ± 2	2 ± 0
5	Number	19.0	1		1	6	2	5	1	3
	%	100	5.2		5.2	31.5	10.4	26.3	5.2	15.7
	% Of total area[a]	–	77.5	–	7.8	11.6	1.2	1.6	0.003	0.006
	Mean size (m^2)		7 370 ± 0	–	745 ± 0	184 ± 18	59 ± 15	30 ± 9	3 ± 0	2 ± 1
10	Number	5.0	1	–	–	1	–	2	1	–
	%	100	20	–	–	20		40	20	
	% Of total area[a]	–	98.3	–	–	1.2	–	0.3	0.06	–
	Mean size (m^2)	–	9 344 ± 0	–	–	118 ± 0	–	17 ± 5	6 ± 0	–

[a] Pixel size was 1 m

[b] Overall weed patch area was 9 502 m^2

[c] Standard deviation

(Blackmore 1996; Kropff et al. 1997). In addition, SARI® software can work with any biotic or abiotic factor that can be discriminated within the remotely sensed image and with the parameters to characterize such factors as the BDV, patch distance and patch sizes.

Most applications of remotely sensed imagery in agriculture require a spatial resolution of less than 10–15 m pixel^{-1}. Generally, the finer the spatial resolution, the more accurate the assessment. Efficient programming of site-specific operations of biotic factors, such as mapping weeds, normally requires spatial resolution of about 1 m or less (López-Granados et al. 2006; Peña-Barragán et al. 2007). Remotely sensed images with spatial resolution from 0.25 to 1.0 m were suitable for olive grove characterization using CLUAS® software (García-Torres et al. 2008b). In this study, remotely sensed imagery with similar spatial resolution has been used with SARI®.

Patchy distribution of weeds in fields has been studied using ground techniques (Krohmann et al. 2006; Ruiz et al. 2006), complemented with geo-statistical approaches (Jurado-Expósito et al. 2003), concluding that weed infestations were concentrated in a few large but unevenly-shaped patches, with a larger number of smaller and more even patches accounting for a small proportion of the infestation. Generally, the weed patch study using SARI® software is in agreement with previous findings. However, patch studies carried out on remote images through SARI® software are much more cost–effective than those achieved through conventional ground techniques.

An important limitation of the SARI system herein described is that weeds or other biotic or abiotic factors have to be discriminated in the remotely sensed image. Referring to weeds, nowadays weed discrimination in crops is mainly restricted to late season species overgrowing the crop with different stages of senescence (López-Granados et al. 2006; Peña-Barragán et al. 2007). However, efforts to discriminate early weed discrimination in crop rows is under development (Gerhards 2010; Ford et al. 2011), which will largely amplify the possibilities of using SARI.

Conclusions

SARI® software splits field plot images into grids composed of rectangular micro-images or micro-plots, whose width and length are defined as multiples of the image spatial resolution. SARI® calculates different indicators for each micro-plot, including the IDV and the %PI with a DV $\neq$ 0; the system also classifies the micro-plots in arbitrarily defined classes based on these indicators. Using SARI®, the key crop characteristics can be spatially assessed from remotely sensed imagery, meeting one basic requirement of precision agriculture: a characterisation of the needs of each small defined area.

SARI® is a practical piece of software for sectioning remotely sensed images, assessing agro-environmental indicators and implementing weed control strategies for each micro-image. The SARI® system provides geo-referenced, quantitative and visual herbicide prescription application maps, and this information could be transferred to variable-rate application equipment for practical SSWM strategies. SARI® can greatly improve and facilitate the use of remote imagery for precision agriculture.

Acknowledgment This research was partially financed by the Spanish Commission of Science and Technology through the projects AGL2007-60926 and AGL2010-15506.

References

Barroso, J., Fernández-Quintanilla, C., Ruiz, D., Hernáiz, P., & Rew, L. J. (2004). Spatial stability of *Avena sterilis* ssp. *ludoviciana* populations under annual applications of low rates of imazamethabenz. *Weed Research, 44*, 178–186.

Barroso, J., Ruiz, D., Fernández-Quintanilla, C., Leguizamón, E. S., Hernaiz, P., Ribeiro, A., et al. (2005). Comparison of sampling methodologies for site-specific management of *Avena sterilis*. *Weed Research, 45*, 1–10.

Blackmore, S. (1996). An information system for precision farming. In *Brighton conference on pests and diseases* (Vol. 3, pp. 1207–1214). Alton, UK: British Crop Protection Council.

Chang, J., Clay, S. A., Clay, D. E., & Kevin, D. (2004). Detecting weed-free and weed-infested areas of a soybean field using near-infrared spectral data. *Weed Science, 52*, 642–646.

Christensen, S., Heisel, T., Walter, A. M., & Graglia, E. (2003). A decision algorithm for patch spraying. *Weed Research, 43*, 276–284.

DeCastro, A., Jurado-Expósito, M., Peña-Barragán, J. M., García-Torres, L., & López-Granados, F. (2009). Classification of *Diplotaxis virgata* and *Sinapis arvensis* in wheat, broad bean and peas using aerial images. In J. L. Gonzalez-Andujar (Ed.), *Proceeding of the II weed science Iberian congress* (Vol. 2, pp. 579–582). Lisbon, Portugal: ISA Press. (in Spanish).

Ford, A. J., Dotray, P. A., Keeling, J. W., Wilkerson, J. B., Wilcut, J. W., & Gilbert, L. V. (2011). Site-specific weed management in cotton using WebHADSS™. *Weed Technology, 25*, 107–112.

García-Torres, L., Gómez-Candón, D., Caballero-Novella, J. J., Gómez-Casero, M., Peña-Barragán, J. M., Jurado-Expósito, M., et al. (2010). Management of remote imagery for precision agriculture. In R. Khosla (Ed.), *10th conference on precision agriculture*. Denver, CO: International Society of Precision Agriculture.

García-Torres, L., López-Granados, F., Peña-Barragán, J. M., Caballero-Novella, J. J., & Jurado-Expósito, M. (24 June 2009). *Automatic procedure to section remote images and to characterize agri-environmental indicators*. PCTES2009/070247. Madrid: Spanish Office for Patents and Trademarks (in Spanish).

García-Torres, L., Peña-Barragán, J. M., Caballero-Novella, J. J., López-Granados, F., & Jurado-Expósito M. (2008a). *SARI® software, splitting and assessment of remote images, Office for the Registration of Intellectual Property*. No. 200899900226820. Seville, Spain: Regional Department of Culture (in Spanish).

García-Torres, L., Peña-Barragán, J. M., López-Granados, F., Jurado-Expósito, M., & Fernández-Escobar, R. (2008b). Automatic assessment of agro-environmental indicators from remotely sensed images of tree orchards and its evaluation using olive plantations. *Computers and Electronics in Agriculture, 61*, 179–191.

Gerhards, R. (2010). Spatial and temporal dynamics of weed populations. In E.-C. Oerke et al. (Eds.), *Precision crop protection—the challenge and use of heterogeneity* (Part 1, pp. 17–25). doi: 10.1007/978-90-481-9277-9_2.

Gibson, K. D., Dirks, R., Medlin, C. R., & Johnston, L. (2004). Detection of weed species in soybean using multispectral digital images. *Weed Technology, 18*, 742–749.

Jordan, C. F. (1969). Derivation of leaf area index from quality of light on the forest floor. *Ecology, 50*, 663–666.

Jurado-Expósito, M., López-Granados, F., García-Torres, L., García-Ferrer, A., Sánchez de la Orden, M., & Atenciano, S. (2003). Multi-species weed spatial variability and site-specific management maps in cultivated sunflower. *Weed Science, 51*, 319–328.

Koger, H. K., Shaw, D. R., Watson, C. E., & Reddy, K. N. (2003). Detecting late-season weed infestations in soybean (*Glycine max*). *Weed Technology, 17*, 696–704.

Krohmann, P., Gerhards, R., & Kühbauch, W. (2006). Spatial and temporal definitions of weed patches using quantitative image analysis. *Journal of Agronomy and Crop Science, 192*, 72–78.

Kropff, M. J., Wallinga, J. & Lotz L. A. P. (1997). Modelling for precision weed management. In G. R. Bock & J. A. Goode (Eds.), *Precision agriculture: Spatial and temporal variability of environmental quality* (pp. 182–204). L. J. Ciba Foundation, Wiley.

Lamb, D. W., & Weedon, M. (1998). Evaluating accuracy of mapping weeds in fallow fields using airborne imaging: *Panicum effusum* in oil-seed rape stubble. *Weed Research, 38*, 443–451.

Lamb, D. W., Weedon, M., & Rew, R. J. (1999). Evaluating the accuracy of mapping weeds in seedling crops using airborne digital imagery: *Avena* spp. in seedling triticale. *Weed Research, 39*, 481–492.

Lancashire, P. D., Bleiholder, H., Van Den Doom, T., Langelüddeke, P., Srauss, R., Weber, E., et al. (1991). A uniform decimal code for growth stages of crops and weeds. *Annals of Applied Biology, 119*, 561–601.

Landis, J. R., & Kock, G. G. (1977). The measurement of observer agreement for categorical data. *Biometrics, 33*, 159–174.

Lass, L. W., & Callihan, R. H. (1997). The effect of phenological stage on detectability of yellow hawkweed (*Hieracium pratense*) and oxeye daisy (*Chysanthemum leucanthemum*) with remote multispectral digital imagery. *Weed Technology, 11*, 248–256.

Lass, L. W., Saffi, B., Price, W. J., & Thill, D. C. (2000). Assessing agreement in multispectral images of yellow starthistle (*Centaurea solstitialis)* with ground truth data using a Bayesian methodology. *Weed Technology, 14*, 539–544.

López-Granados, F., Jurado-Expósito, M., Peña-Barragán, J. M., & García-Torres, L. (2006). Using remote sensing for identification of late-season grass weed patches in wheat. *Weed Science, 54*, 346–353.

MARM. (2011). Spanish Ministry of Environment, Rural and Marine. http://www.marm.es/es/estadistica/temas/encuesta-sobre-superficies-y-rendimientos-de-cultivos-esyrce-/. Madrid, Spain. Last Accessed 11 June 2011 (in Spanish).

Medlin, C. R., Shaw, D. R., Gerard, P. D., & Lamastus, F. E. (2000). Using remote sensing to detect weed infestations in *Glycine max*. *Weed Science, 48*, 393–398.

Peña-Barragán, J. M., López-Granados, F., Jurado-Expósito, M., & García-Torres, L. (2007). Mapping *Ridolfia segetum* patches in sunflower (*Helianthus annuus L.*) crop using remote sensing. *Weed Research, 47*, 164–172.

Rouse, J. W., Hass, R. H., Schell, J. A., & Deering, D. W. (1973). Monitoring vegetation systems in the Great Plains with ERTS. In RJW & RS (ed.), *Proceedings of the earth research technology satellite symposium* (Vol. 1, pp. 309–317). NASA SP-351.

Ruiz, D., Escribano, C., & Fernández-Quintanilla, C. (2006). Assessing the opportunity for site-specific management of *Avena sterilis* in winter barley fields in Spain. *Weed Research, 46*, 379–387.

Saavedra, M., Cuevas, J., Mesa-García, J., & García-Torres, L. (1989). Grassy weeds in winter cereals in Southern Spain. *Crop Protection, 88*, 181–187.

Thomlinson, J. R., Bolstad, P. V., & Cohen, W. B. (1999). Coordinating methodologies for scaling land-cover classifications from site-specific to global: steps toward validating global map product. *Remote Sensing of the Environment, 70*, 16–28.

Thompson, J. F., Stafford, J. V., & Miller, P. C. H. (1991). Potential for automatic weed detection and selective herbicide application. *Crop Protection, 10*, 254–259.

Thorp, K. R., & Tian, L. F. (2004). A review of remote sensing of weeds in agriculture. *Precision Agriculture, 5*, 477–508.

Timmermann, C., Gerhards, R., & Kühbauch, W. (2003). The economic impact of site-specific weed control. *Precision Agriculture, 4*, 249–260.

Vrindts, E., Baerdemaeker, J. D., & Ramon, H. (2002). Weed detection using canopy reflection. *Precision Agriculture, 3*, 63–80.

Wilson, B. J., & Brain, P. (1991). Long-term stability of distribution of *Alopecurus myosuroides* Huds. within cereal fields. *Weed Research, 31*, 367–373.